Implementation of fuzzy controller for measuring instantaneous arterial blood pressures via tissue control method

A.C.-Y. Lin, H.-N. Huang, Y.-C. Su, C.-Y. Shiu and J.-L. Hwang

Abstract: A fuzzy controller to implement tissue control method (TCM) proposed by Lin *et al.* (in physiol Meas, 2006) to measure the instantaneous arterial blood pressure is presented. The TCM adopts a piezo-actuator to move the pressure transducer up and down to maintain the mean blood pressure measured on the skin by tracking the variation in the blood pressure. Since the operation of the piezo-actuator exhibits hysteresis behaviour in the actuator movement, the controller should have the ability to track the blood pressure variation as well as compensate for the hysteretic movement. A Takagi–Sugeno fuzzy model is adopted to represent the Bouc–Wen model in describing the hysteresis with parameters identified from the dynamic responses of the actuator. On the basis of the model, a stable fuzzy observer is developed to linearise the movement of the piezo-actuator, and a PI controller is designed to track the variation in blood pressure. The designed fuzzy controller has successfully tracked various command signals during software and hardware tests. The fuzzy controller is located in an instrument that measures the instantaneous blood pressure. The experimental results show that the proposed fuzzy controller is feasible and satisfactory for controlling the piezo-actuator.

1 Introduction

The study of using the blood pressure cuff and Korotkoff sounds to design auscultatory sphygmomanometry has been conducted over a century, and have been many sphygmomanometry devices introduced for medicine and daily heath care purposes [1–5]. The development of non-invasive measurements for blood pressure has been discussed in Yamakoshi [6] and the references therein. Unfortunately, because of the significance of arterial blood pressure, it is still difficult to obtain the actual value of instantaneous blood pressure in the artery, because the characteristics of blood pressure cannot be transmitted from inside the artery to the skin. To the best of our knowledge, only very limited devices, such as the non-invasive-type device reported by Tanaka *et al.* [7], the finometer by Finapres Medical Systems and the HDI/PulseWave^{TM} CR-2000 by Hypertension Diagnostics Inc., can provide blood pressure waveform for research purposes and clinical studies. After conducting many animal experiments, Lin *et al.* [8] recently proposed a compliance model and then developed a new technique to calculate the instantaneous blood pressure based on the so-called tissue control method (TCM) [8]. The aim of the TCM is to keep the compliance of the tissue unchanged as the arterial blood pressure varies. This is done by tracking the variation of the arterial blood pressure by moving the actuator. In order to actualise the TCM, a fuzzy controller is designed to control the motion of the piezo-type actuator. This paper reveals the implementation of this fuzzy observer to overcome the nonlinearity in the piezo-actuator and in the skin, tissue and blood vessel.

Before designing the controller, we must build a mathematical model to describe the nonlinear behaviour of peizo-actuators. The Bouc–Wen model [9], which belongs to the class of endochronic models, has been widely used to describe hysteretic behaviour. This model consists of a system of nonlinear differential equations where the memory-dependent nature of hysteresis is taken into account by using an extra variable. Various values of the parameters of this model reveal a wide range of mechanical behaviour. With appropriate parameters determined by the identification algorithm on experimental data, it is possible to describe sufficiently the nonlinear dynamic behaviour of a hysteretic system. To overcome the difficulty of designing the controller for a nonlinear system, the Tukagi–Sugeno (T–S) fuzzy model will approximate the nonlinear system by smoothly interpolating affine local models [10]. Each local model contributes to the global model in a fuzzy subset, which is characterised by a membership function. Once the T–S fuzzy model for the hysteretic dynamics of the piezo-actuator is built, the robust fuzzy observer is carried by the parallel-distributed compensation (PDC) control scheme [11]. The design of PDC control scheme consists of two steps: The first is to derive each control rule corresponding to each linear model in the T–S fuzzy model and the second to generate the overall fuzzy controller by blending all of the individual linear controllers. By converting these stability requirements for controller design into linear matrix inequality (LMI)

doi:10.1049/iet-cta:20060530

Paper first received 20th December 2006 and in revised form 21st May 2007

A.C.-Y. Lin, C.-Y. Shiu and J.-L. Hwang are with the Department of Automatic Control Engineering, Feng Chia University, Taichung, Taiwan 407, Republic of China

H.-N. Huang is with the Department of Mathematics, Tunghai University, Taichung, Taiwan 407, Republic of China

Y.-C. Su is with the School of Chinese Medicine, China Medical University, Taichung, Taiwan 405, Republic of China

E-mail: nhuang@thu.edu.tw

conditions [12], many effective algorithms can be used to find the feedback gain for the fuzzy observer [13].

Using this process, we develop a fuzzy observer for a piezo-actuator PST 150/5 made by Piezolechanhk, Inc. Then, a proportional-integral (PI) controller is used to track the variation in the blood pressure on the skin. Combining these two parts, a fuzzy control to implement the TCM is obtained and verified using software simulation and hardware testing. From the verification test, it was found that there are still some discrepancies between the expected and real output signals because of the time-delay effect associated with the mechanical behaviour of the actuator. Fourier series analysis is used to reduce the discrepancies via delay-time compensation in each frequency mode. Finally, the controller to the is incorporated in the instrument for non-invasive measurement of instantaneous arterial blood pressure. The experiment shows that this fuzzy control is feasible and shows satisfactory results.

2 Basic theory and method

In this section, we review background information of TCM and the basic theory related to modelling the nonlinear behaviour of piezo-actuators and fuzzy controller design.

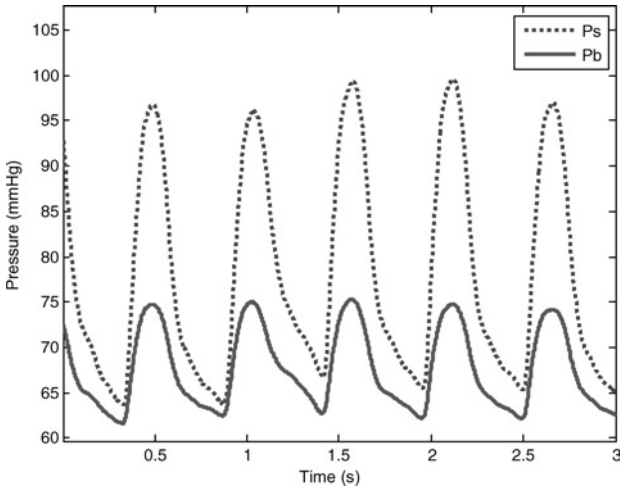

Fig. 1 *Typical blood pressures measured on the skin and inside the arterial vessel, respectively*

2.1 Transmission characteristics and equivalent compliance

To understand the transmission characteristics of blood pressure from inside the artery to the skin above, e-Med Biotech Inc. and ATIT (Animal Technology Institute Taiwan) conducted a series of animal (pig) experiments (for more detailed information, see [6]). Fig. 1 shows the two typical blood pressures measured on the skin with 6 mm pressed depth and inside the arterial vessel, denoted by P_s and P_b, with the Grass Telfactor P10EZ pressure transducer. By analysing the experimental data, Lin *et al.* [8] proposed a series of compliance models of the femoral artery in steady-state conditions (Fig. 2) to explain the transmission mechanism of blood pressure which includes the skin, tissue and arterial vessel. According to circuit theory and $R_t = R_{t1} + R_{t2}$, the measured compliance, R_s, on the skin is given by

$$\frac{\lambda_s}{P_s} = R_s = R_t + R_v\left(1 - \frac{P_b}{P_s}\right) \tag{1}$$

where λ_s is the pressed depth, and $R_t(=R_{t1} + R_{t2})$ and R_v denote the impedances (compliances) of tissue and blood vessel, respectively.

2.2 Tissue control method

Obviously, (1) states that there exists a location $\bar{\lambda}_s$ where the arterial blood pressure, P_b, is equal to the skin blood pressure, P_s. It was shown in [8] that these pressures are recognised as the mean arterial blood pressure (MBP), $\bar{P}_b$, and the mean blood pressure measured on the skin (MSP), $\bar{P}_s$. The existence of such a location reveals three facts: first, the measured compliance R_s is equal to the compliance of tissue R_t only, the compliance of the blood vessel is not involved; secondly, if this particular compliance R_t is maintained as the arterial blood pressure varies from MBP by moving the pressed depth, the variation in blood vessel diameter can be obtained; thirdly, since the variation in arterial blood pressure must be tracked to maintain the MBP, it is possible to obtain the instantaneous arterial blood pressure.

To independently stimulate the activity of the blood vessel, TCM [8] obtains the variation of blood vessel diameter by maintaining the mean blood pressure and tracking the variation of arterial blood pressure. After recognising the compliances of the tissue and the blood vessel, it then

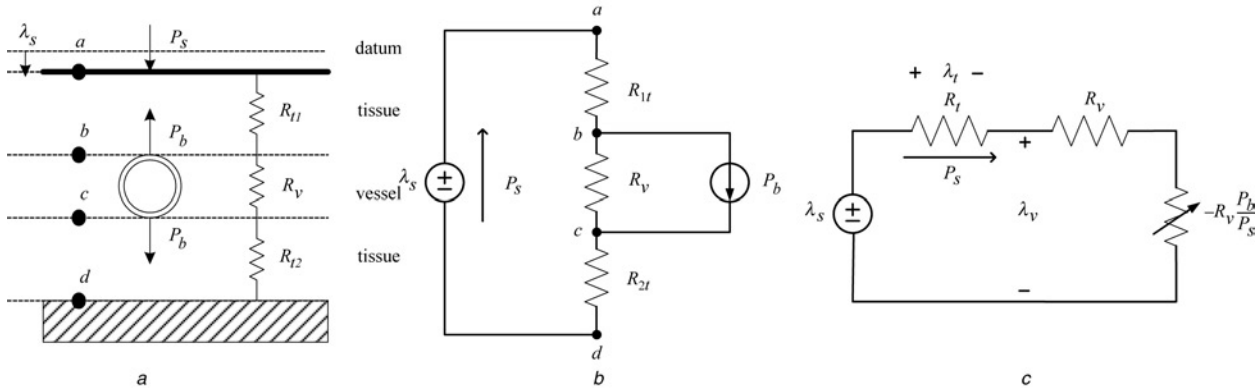

Fig. 2 *Series of compliance models of the femoral artery*

a Physical model
b Lumped compliance circuit
c Equivalent compliance circuit

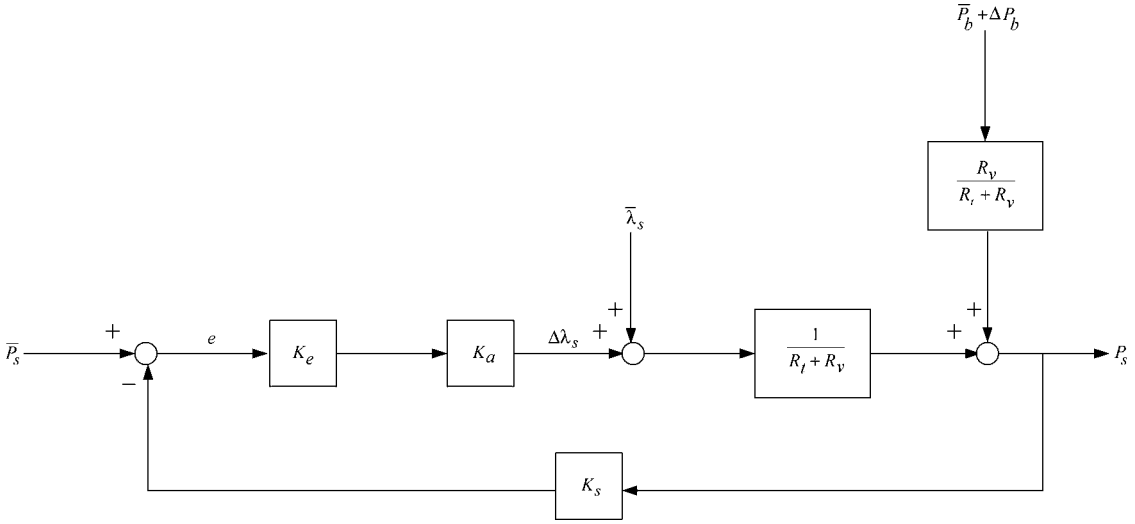

Fig. 3 *Schematic diagram for tissue control method*

computes the instantaneous arterial blood pressure. Fig. 3 shows the schematic diagram that keeps the measured compliance equal to the tissue compliance.

At $\bar{\lambda}_s$, MBP is equivalent to MSP and hence (1) leads to

$$\frac{\bar{\lambda}_s}{\bar{P}_s} = R_t \tag{2}$$

Let ΔP_b and ΔP_s represent increases in $\bar{p}_b$ and $\bar{p}_s$, respectively. When ΔP_b increases, the actuator will move up, $\Delta\lambda_s$, from $\bar{\lambda}_s$ to maintain the MBP, by creating an error pressure ΔP_s to drive the controller. Then, from the the TCM, shown in (Fig. 3) one obtains

$$\bar{P}_s = \frac{1}{R_t + R_v}(\bar{\lambda}_s + \Delta\lambda_s) + \frac{R_v}{R_t + R_v}(\bar{P}_b + \Delta P_b) \tag{3}$$

The substitution of (3) into (2) gives us

$$\Delta\lambda_s = -R_v \Delta P_b \tag{4}$$

Recalling the mechanism depicted in Fig. 2, (4) interprets that the displacement of actuator $\Delta\lambda_s$ is the variation of the blood vessel diameter. Then, the instantaneous arterial blood pressure, P_b, could be computed by

$$P_b = \bar{P}_b + \Delta P_b = \bar{P}_s - \frac{R_t + R_v}{R_v}\Delta P_s \tag{5}$$

2.3 T–S fuzzy model

In order to estimate the instantaneous arterial blood pressure using TCM, we must incorporate an actuator that can perform a 100-μm stroke with precision within 0.1 μm; the response time should be <1 ms and bandwidth of the signals is <10 Hz.

Owing to its light weight, small size, high rigidity and high precision, the piezo-actuator Pst 150/5/100 has been adopted in our system to perform tissue-control pressure-tracking and to collect the required signals. In order to overcome the hysteresis and delay nonlinearity of the piezo material, we present the Bouc–Wen model and use the T–S fuzzy rule to approximate this nonlinear model by smoothly interpolating an affine linear local model.

2.3.1 Bouc–Wen model: To understand the nonlinear effect of the actuator's hysteresis, the triangular wave signal as shown in Fig. 4*a* is used to test the actuator's response with three different peak-to-peak amplitudes at 150, 75 and 37.5 V. The displacement output of the actuator corresponding to the 150-V input is depicted in Fig. 4*b*. Fig. 5 shows the phase plot of the displacement against input voltage with respect to input signals. There are three

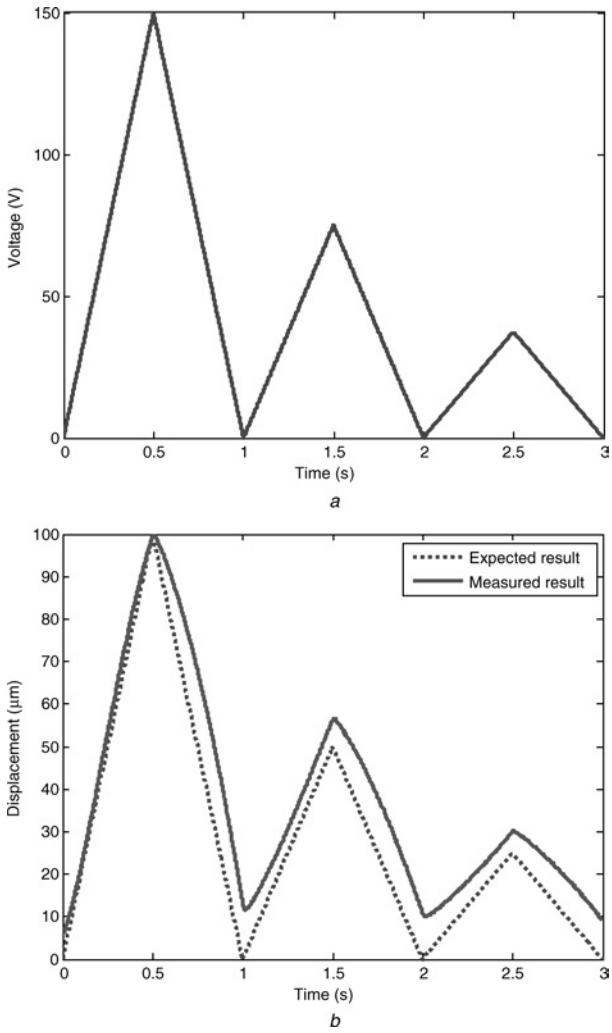

Fig. 4 *Comparison between input and output signals of the piezo-actuator*

a Wave shape of command input signal
b Expected and measured displacement output signals

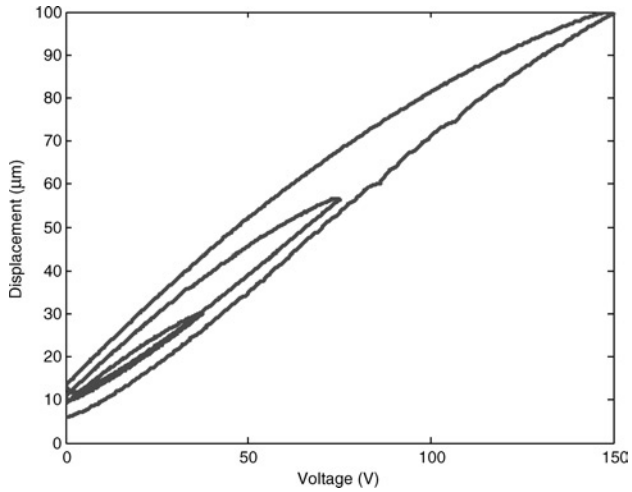

Fig. 5 *Displacement variation of the actuator with respect to different input voltages*

hysteresis loops in Fig. 5 that correspond to input signals with 150, 75 and 37.5 peak-to-peak voltages, respectively. After further experiments, the number of loops is related to the wave shape, amplitude and frequency of the input signals and Bouc–Wen type mathematical model is developed to model the hysteresis.

Let x, u and h denote the actuator displacement, input voltage and hysteresis parameter, respectively. Their mathematical relationship is given by

$$m\ddot{x} + b\dot{x} + kx = k(du - h) \tag{6a}$$

$$\dot{h} = \alpha d\dot{u} - \beta|\dot{u}|h - \gamma\dot{u}|h| \tag{6b}$$

where m, b and k are mass, damping and stiffness of the actuator. Equation (6b) describes hysteresis behaviour, which is denoted by h with the same unit as the displacement and is parameterised with coefficients α, β and γ.

2.3.2 Discrete state–space representation of Bouc–Wen model: Let T denote the sample period and $f(k)$ denote $f(kT)$ to represent $f(t)$ for $t \in [kT,\ kT+T)$. Using a standard discretisation procedure, the discrete state–space representation of (6) is obtained as

$$\begin{bmatrix} x_1(n+1) \\ x_2(n+1) \\ h(n+1) \end{bmatrix} = \begin{bmatrix} a_{11} & a_{12} & -\dfrac{b_1}{d} \\ a_{21} & a_{22} & -\dfrac{b_2}{d} \\ 0 & 0 & \dfrac{1-\beta/2|v(n)|}{1+\beta/2|v(n)|} \end{bmatrix} \begin{bmatrix} x_1(n) \\ x_2(n) \\ h(n) \end{bmatrix} + \begin{bmatrix} b_1 \\ b_2 \\ 0 \end{bmatrix} u(n) + \begin{bmatrix} 0 \\ 0 \\ \dfrac{\alpha d}{1+\beta/2|v(n)|} \end{bmatrix} v(n) \tag{7}$$

where $v(n) = u(n+1) - u(n)$

$$\begin{bmatrix} a_{11} & a_{12} \\ a_{21} & a_{22} \end{bmatrix} = e^{AT}, \quad A = \begin{bmatrix} 0 & 1 \\ -\dfrac{k}{m} & -\dfrac{b}{m} \end{bmatrix} \quad \text{and} \quad \begin{bmatrix} b_1 \\ b_2 \end{bmatrix} = \left(\int_0^T e^{A\lambda} \mathrm{d}\lambda\right) B, \quad B = \begin{bmatrix} 0 \\ -\dfrac{kd}{m} \end{bmatrix}$$

2.3.3 T–S fuzzy model: The T–S fuzzy model [8] has the following IF–THEN form in representing a discrete fuzzy system (DFS) to describe a linear operating segment of a discrete nonlinear system

Model Rule i:
IF $z_1(t)$ is M_{i1} and $\cdots$ and $z_p(t)$ is M_{ip},
THEN $x(t+1) = A_i x(t) + B_i u(t)$, $y(t) = C_i x(t)$, $\quad i = 1, 2, \ldots, r.$

Given a pair of $(x(k), u(k))$, the final output of the T–S fuzzy model is inferred as follows

$$x(t+1) = \frac{\sum_{i=1}^{r} w_i(z(t))\{A_i x(t) + B_i u(t)\}}{\sum_i^r w_i(z(t))}, \qquad y(t) = \frac{\sum_{i=1}^{r} w_i(z(t)) C_i x(t)}{\sum_i^r w_i(z(t))} \tag{8}$$

where $z(t) = [z_1(t)\ \ z_2(t)\ \ \cdots\ \ z_P(t)]$ and

$$w_i(z(t)) = \prod_{j=1}^{P} M_{ij}(z_j(t)), \qquad h_i(z(t)) = \frac{w_i(z(t))}{\sum_{i=1}^{r} w_i(z(t))} \geq 0, \quad \sum_{i=1}^{r} h_i(z(t)) = 1 \tag{9}$$

for all t, with $M_{ij}(z_j(t))$ denoting the ith membership function corresponding to $z_j(t)$.

2.4 Fuzzy observer design

Considering the fuzzy model (8), a fuzzy controller is designed on the basis of PDC concepts so as to share the same fuzzy sets with the plant. First, an observer is constructed with the requirement that $x(t) - \hat{x}(t) \to 0$ when $t \to \infty$, that is, no steady-state error. Here, $\hat{x}$(t) is the estimated state from the observer. The PDC-type fuzzy observer is described as

Observer Rule i:
IF $z_1(t)$ is M_{i1} and $\cdots$ and $z_p(t)$ is M_{ip},
THEN $\hat{x}(t+1) = A_i\hat{x}(t) + B_i u(t) + K_i(y(t) - \hat{y}(t))$, $\hat{y}(t) = C_i\hat{x}(t)$, $\quad i = 1, 2, \ldots, r$

where K_i is the local observer gain. The output of the PDC-type fuzzy observer is determined by

$$u(t) = -\frac{\sum_{i=1}^{r} w_i(z(t)) F_i \hat{x}(t)}{\sum_{i=1}^{r} w_i(z(t))} = -\sum_{i=1}^{r} h_i(z(t)) F_i \hat{x}(t) \tag{10}$$

Substituting (10) into (8), one can obtain the corresponding closed-loop discrete T–S fuzzy model with $e(t) = x(t) - \hat{x}(t)$ denoting the error between actual and observer states.

$$x(t+1) = \sum_{i=1}^{r}\sum_{j=1}^{r} h_i(z(t))\, h_j(z(t))\, \{(A_i - B_i F_j)\, x(t) + B_i F_j\, e(t)\} \tag{11}$$

$$e(t+1) = \sum_{i=1}^{r}\sum_{j=1}^{r} h_i(z(t)) h_j(z(t)) \{A_i - K_i C_j\} e(t) \tag{12}$$

Let $x_a = [x \ e]^T$, and the combination of (11) and (12) then leads to

$$x_a(t+1) = \sum_{i=1}^{r}\sum_{j=1}^{r} h_i(z(t))h_j(z(t))G_{ij}x_a(t)$$

$$= \sum_{i=1}^{r} h_i(z(t))h_i(z(t))G_{ii}x_a(t) \quad (13)$$

$$+ 2\sum_{i=1}^{r}\sum_{i<j} h_i(z(t))h_j(z(t))\frac{G_{ij}+G_{ji}}{2}x_a(t)$$

where

$$G_{ij} = \begin{bmatrix} A_i - B_iF_j & B_iF_j \\ 0 & A_i - K_iC_j \end{bmatrix}$$

To satisfy the global stability requirement, there must exist a positive definite matrix P such that

$$G_{ii}^T P G_{ii} - P < 0 \quad (14a)$$

$$\left(\frac{G_{ij}+G_{ji}}{2}\right)^T P\left(\frac{G_{ij}+G_{ji}}{2}\right) - P < 0, \quad i<j \text{ s.t. } h_i \cap h_j \neq \phi \quad (14b)$$

To compute the matrix P so as to calculate the optimal feedback gain F_i and observer gain K_i, we put all these equations into an LMI form. By defining $M_{1i} = F_iP_1$ and $N_{2i} = P_2K_i$ we then arrive at the final LMIs via Schur complements.

$$P_1, P_2 > 0, \begin{bmatrix} P_1 & P_1A_i^T - M_{1i}^TB_i^T \\ A_iP_1 - B_iM_{1i} & P_1 \end{bmatrix} > 0,$$

$$\begin{bmatrix} P_2 & A_i^TP_2 - C_i^TN_{2i}^T \\ P_2A_i - N_{2i}C_i & P_2 \end{bmatrix} > 0$$

$$\begin{bmatrix} 4P_1 & (P_1A_i^T - M_{1j}^TB_i^T + P_1A_j^T - M_{1i}^TB_j^T) \\ (A_iP_1 - B_iM_{1j} + A_jP_1 - B_jM_{1i}) & P_1 \end{bmatrix} > 0$$

$$\begin{bmatrix} 4P_2 & (A_i^TP_2 - C_j^TN_{2i}^T + A_j^TP_2 - C_i^TN_{2i}^T) \\ (P_2A_i - N_{2i}C_j + P_2A_i - N_{2i}C_j) & P_2 \end{bmatrix} > 0$$

which are solved using an optimisation technique like the LMI method [11].

3 Controller design and implementation

3.1 Controller design

Since Pst 150/5/100 exhibits a hysteresis loop in the displacement variation during operation, a T–S fuzzy model is developed as shown in Section 2.3 to describe the nonlinear behaviour of hysteretic movement. The controller for this actuator consists of two parts: one is a simple PI controller and the other is a fuzzy observer. The fuzzy observer is designed to linearise the movement of the piezo-actuator, whereas the PI controller is used to track the variation of the blood pressure as well. The schematic block diagram of the fuzzy controller is shown in Fig. 6.

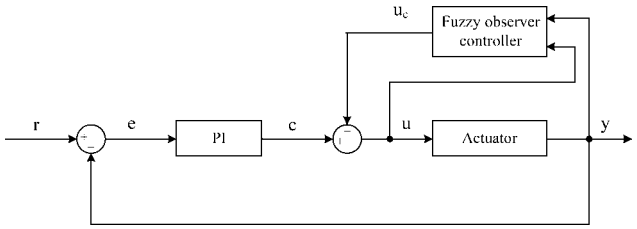

Fig. 6 *Schematic block diagram of the fuzzy controller*

A threshhold is applied to restrict the magnitude of the input signal to the actuator for safe operation. Using the standard system identification technique, the corresponding parameters of the Bouc–Wen model for the actuator are determined to be $\alpha = 0.3$, $\beta = 0.085$, $d = 0.31$. For Pst 150/5/100, the parameters in (6) are verified and listed (in which the parameter γ can be omitted) in Table 1.

To design the PI controller, we need the linear version of the actuator; the transfer function for the linear behaviour of the actuator is given by

$$G(s) = \frac{11683.2}{s^2 + 118.3s + 6637}$$

and the discrete version using zero-order hold with sampling time 0.002 ms is

$$G(z^{-1}) = \frac{0.002158z^{-1} + 0.001994z^{-2}}{1 - 1.766z^{-1} + 0.7893z^{-2}}$$

The PI controller is then designed which leads to the gains $K_p = 1$, $K_i = 125$, and hence its transfer function is

$$G_{PI}(s) = \frac{s + 125}{s}$$

The use of backward Euler method with the sample time 0.002 ms gives us the discrete PI controller.

$$G_{PI}(z^{-1}) = \frac{(1 + 125T) - z^{-1}}{1 - z^{-1}}$$

The discrete version of nonlinear hysteresis behaviour of the actuator is described in (7). Assume $|v(n)| \in [0, a]$ and let

$$P(n) = \frac{1 - (\beta/2)|v(n)|}{1 + (\beta/2)|v(n)|}, \quad X = \frac{1 - (\beta/2)a}{1 + (\beta/2)a}$$

then the function $P(n)$ can be expressed as the combination of membership functions.

$$P(n) = M_1(P(n)) \cdot \left(\frac{1 - (\beta/2)a}{1 + (\beta/2)a}\right) + M_2(P(n)) \cdot 1 \quad (15)$$

where membership functions $M_1(P(n))$, $M_2(P(n)) \in [0, 1]$ must satisfy the relation

$$M_1(P(n)) + M_2(P(n)) = 1 \quad (16)$$

Table 1: Piezo-actuator parameters

m	0.28 kg	α	0.3
b	33.124 N s/m	β	0.085
k	1858.4 N/m	γ	0
d	0.31 μm/V		

and hence they have the following explicit representations

$$M_1(P(n)) = \frac{P(n)-1}{X-1}, \quad M_2(P(n)) = \frac{P(n)-X}{1-X}$$

Therefore the nonlinear T–S fuzzy model of the actuator is

$$\begin{aligned} &\textit{Model Rule } i \\ &\textit{IF } v(t) \textit{ is } M_i \\ &\textit{THEN } \begin{array}{l} x(n+1) = A_{si}x(n) + B_{si}u(t) \\ y(n) = C_{si}x(n) \end{array} \end{aligned}$$

where $i = 1, 2$ and the corresponding matrices are given below

$$A_{s1} = \begin{bmatrix} 0.98774 & 0.0017731 & -2.0884 \\ -11.768 & 0.77798 & -2004.8 \\ 0 & 0 & 1 \end{bmatrix},$$

$$A_{s2} = \begin{bmatrix} 0.98774 & 0.0017731 & -2.0884 \\ -11.768 & 0.77798 & -2004.8 \\ 0 & 0 & 0.95982 \end{bmatrix}$$

$$B_{s1} = \begin{bmatrix} 0.64742 & 0 \\ 621.48 & 0 \\ 0 & 0.093 \end{bmatrix}, \quad B_{s2} = \begin{bmatrix} 0.64742 & 0 \\ 621.48 & 0 \\ 0 & 0.091132 \end{bmatrix}$$

$$C_{s1} = \begin{bmatrix} 1 & 0 & 0 \end{bmatrix}, \quad C_{s2} = \begin{bmatrix} 1 & 0 & 0 \end{bmatrix}$$

The observer gains are computed using the LMI toolbox [11] of MATLAB and are listed as

$$F_1 = \begin{bmatrix} 0.82451 & 0.0024469 & -3.2254 \\ -1407.6 & -2.8351 & 9.0564 \end{bmatrix},$$

$$F_2 = \begin{bmatrix} 0.82133 & 0.00244 & -3.2254 \\ -1429.5 & -2.8652 & 8.877 \end{bmatrix}$$

$$K_1 = \begin{bmatrix} 2.6567 \\ 972.51 \\ -0.2274 \end{bmatrix}, \quad K_2 = \begin{bmatrix} 2.6495 \\ 969.3 \\ -0.21863 \end{bmatrix}$$

3.2 Verification test

In order to verify the effect of the fuzzy controller (including a PI controller and a fuzzy observer) in reducing the

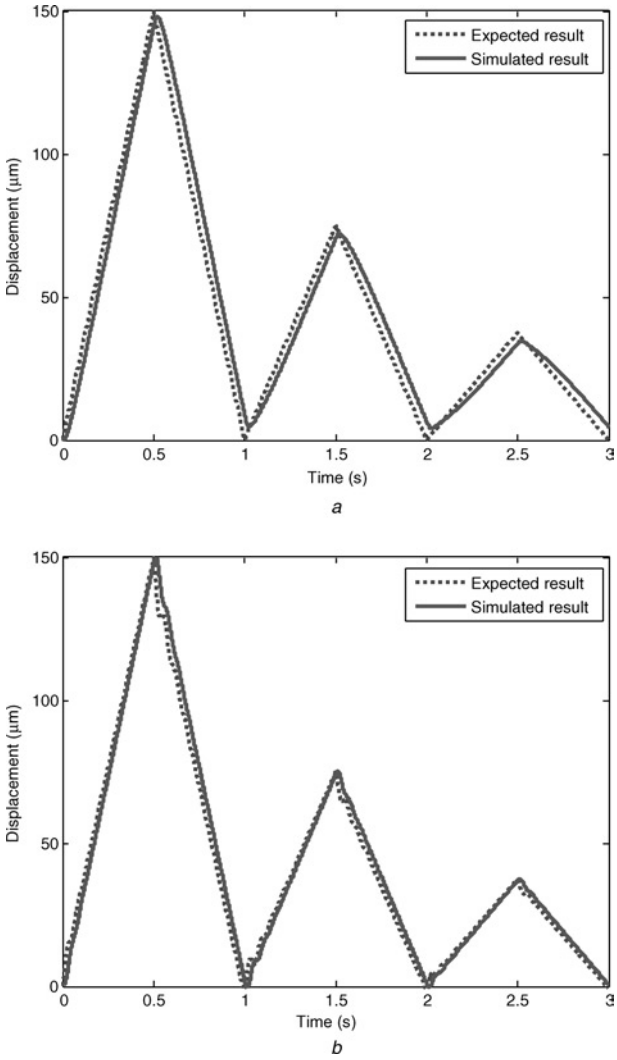

Fig. 7 *Expected and simulation displacement output signals with and without fuzzy controller*

a Without fuzzy controller
b With fuzzy controller

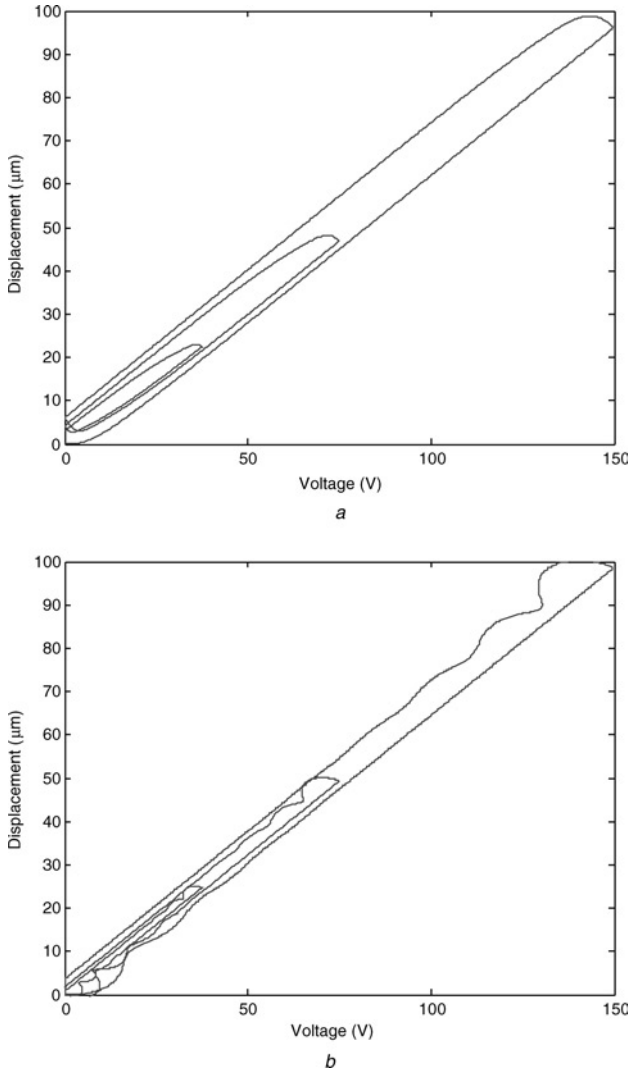

Fig. 8 *Displacement variation against the input voltage of the actuator with and without fuzzy controller*

a Without fuzzy controller
b With fuzzy controller

nonlinearity of the hysteresis behaviour of the piezo-actuator, we perform the following software and hardware tests.

3.2.1 Software verification: In order to verify the effect of the fuzzy controller (including a PI controller and a fuzzy observer) design for the actuator, a software test is built using the SIMULINK in MATLAB. First, we test the effect of the T–S fuzzy model by inputting a triangular wave as shown in Fig. 4*a*, and the corresponding displacement output of the model is given in Fig. 7*a*. The combination of Figs. 4*a* and 7*a* leads to Fig. 8*a*, which shows the variation of the displacement output against input voltages. Compared with the result of the hardware measurement shown in Fig. 5, the T–S model could reproduce the behaviour of the piezo-actuator except in the high-voltage range. To understand the ability of the fuzzy controller in reducing the hysteresis of the piezo-actuator, the same input signal as shown in Fig. 4*a* is supplied and the output is given in Fig. 7*b*. Fig. 8*b* shows the variation of displacement output against different input voltage. From Fig. 8*a* and *b*, the improvement of the hysteresis behaviour is quite evident.

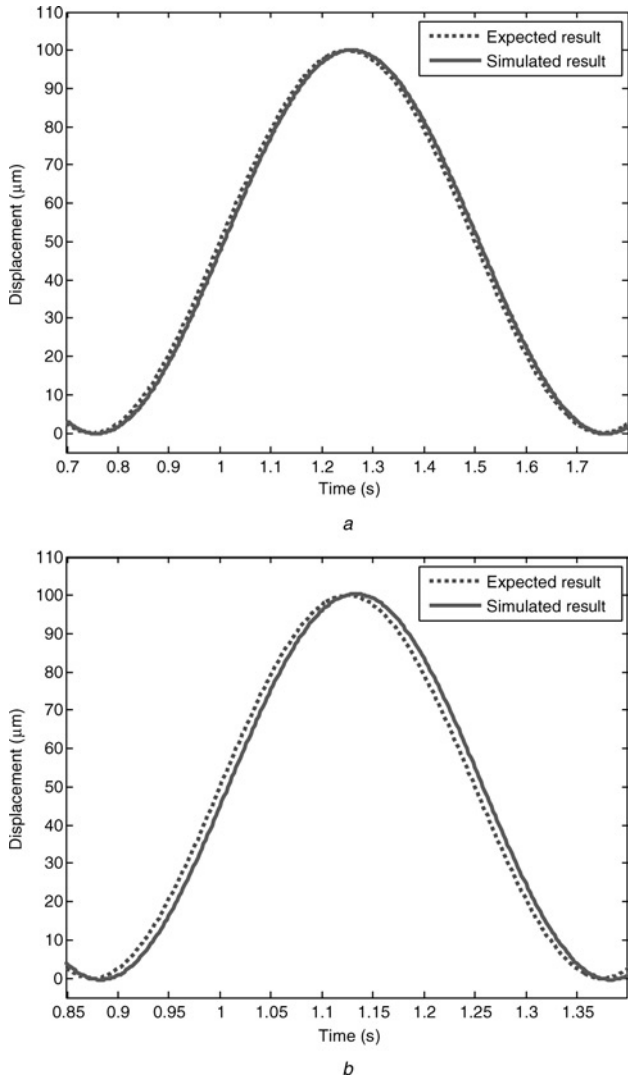

Fig. 9 *Comparison of expected and simulated output signals in software testing*

a 1 Hz sinusoidal output signal
b 2 Hz sinusoidal output signal

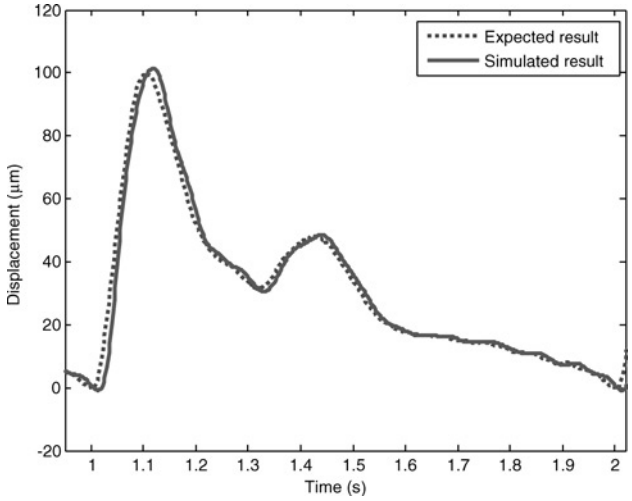

Fig. 10 *Simulation result for the input signal with the shape of the pulse wave of blood pressure*

Fig. 9 gives the displacement outputs corresponding to the 1 and 2 Hz sinusoidal input signals to our T–S model. The root means square (RMS) errors of the expected and simulated signals are 1.7 and 3.5%, respectively. This indicates that when the frequency of the input signal increases, the error increases as well, which results from the time lag between the expected and simulated outputs. To understand the usability in measuring the blood pressure, a pulse wave of blood pressure type reference signal is input to the actuator for test purposes. The corresponding output is depicted in Fig. 10 with 3.5% RMS error. It is evident that the time delay phenomenon varies when the frequency of the input signal is changing.

Although the nonlinear hysteresis behaviour of the actuator has been linearised, but after integration with the fuzzy controller, the overall control system still presents nonlinear phenomena. In order to reduce the error, we apply Fourier series analysis to the output signal shown in Fig. 10, which shows that the response time delay in the first seven modes contributes significantly to the error. Thus, we set the input signals to sinusoidal waves with the frequencies corresponding to the first eight modes of the output signal and then compute the time lag for each

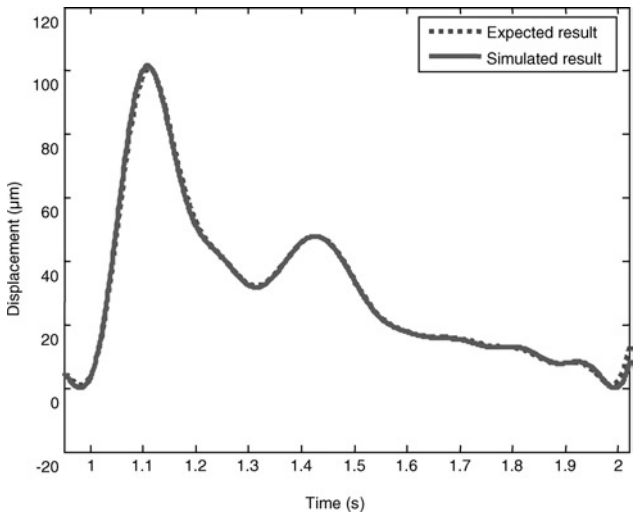

Fig. 11 *Error reduction using Fourier series for delay compensation in software testing*

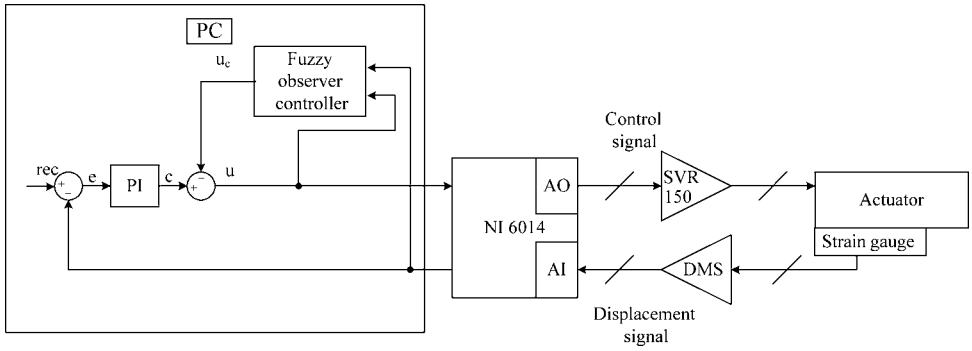

Fig. 12 *Schematic diagram for hardware verification test*

mode via software simulation. After identifying the delay time in each mode, we compensate the delay in each mode (Fig. 11), which reduces the RMS error from 3.5 to 1.57%.

3.2.2 Hardware verification: The hardware architecture for hardware verification is shown in Fig. 12, which includes a PC, NI6014 AD/DA converter, SVR 150 amplifier, actuator Pst 150/5/100 and DMS strain gauge. Resolution of the NI6014 for both A/D and D/A conversions is 16 bits. The associated hardware specifications of these test elements are listed in Table 2.

Fig. 13 shows the corresponding outputs when 1 and 2 Hz sinusoidal waves are chosen as the reference input signals for the hardware test. The errors between the expected and actual output signals are 1.2 and 2.3% for 1 and 2 Hz inputs, respectively. Comparing with the result of the software test, the error is smaller than the corresponding one in the software simulation. The effect of tracking a pulse wave of blood pressure type reference input signal is shown in Fig. 14. The associated RMS error is 2.9% and it is also smaller than the software test.

Table 2: Hardware specifications

Actuator	Amplifier	Strain gauge displacement
type: Pst 150/5/100 VS10	type: SVR 150/3	output:
max. stroke: 130/100 μm	input	0/5 V equivalent piezo actuator's max. strain
length: 100 mm	signal: +/−5 V	
el. capacitance: 4000 nF	impedance: 5 kOhms	impedance: 1 kΩ
stiffness: 5 N/μm	output	
resonance frequency: 10 kHz	voltage total: −30 to +150 V	
	DC-offset range: −30 to +150 V	
	gain: 30	
	max. current: 60 mA	
	noise: 0.3 mVpp (for 4.7 μF load)	

Fourier series analysis is applied to reduce the delay effect, and the resulting output response is shown in Fig. 15; as can be seen, the RMS error has reduced from 2.9 to 0.4%.

From the results of software and hardware testing, the PI controller and fuzzy observer incorporated with the piezo-actuator presents a satisfactory tracking performance for the application of the TCM.

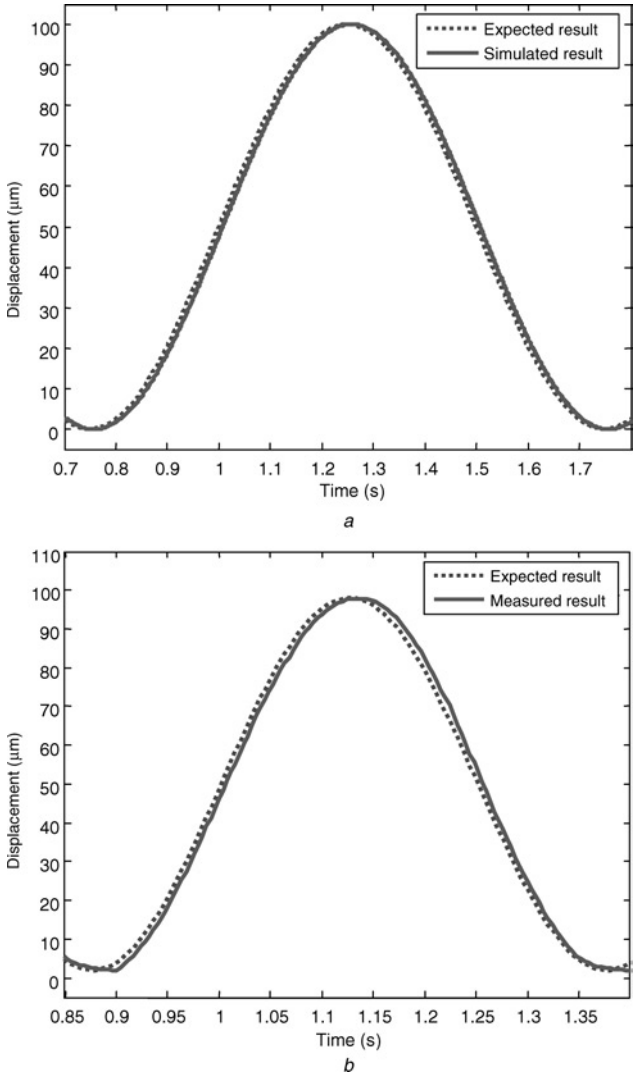

Fig. 13 *Comparison between expected and measured output signals for hardware testing*

a 1 Hz sinusoidal output signal
b 2 Hz sinusoidal output signal

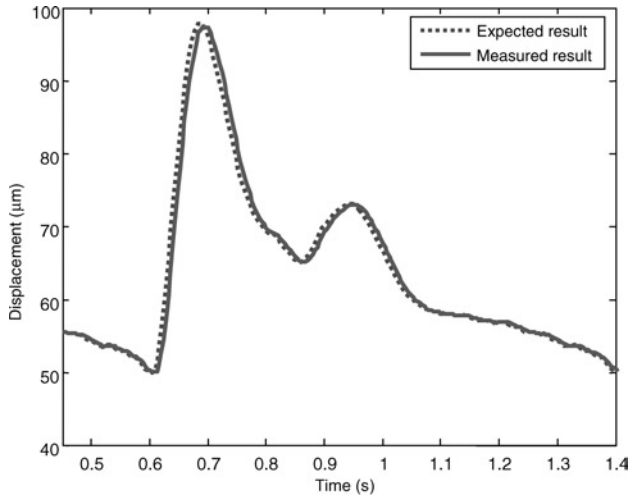

Fig. 14 *Tracking effect on a pulse wave of blood pressure type*

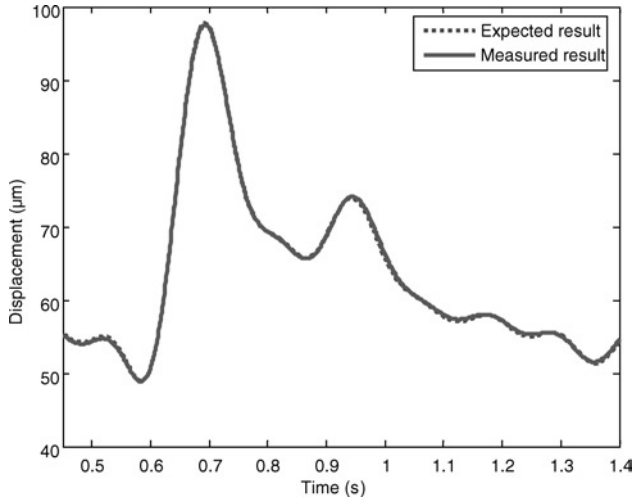

Fig. 15 *Error reduction using Fourier series for delay compensation in hardware test*

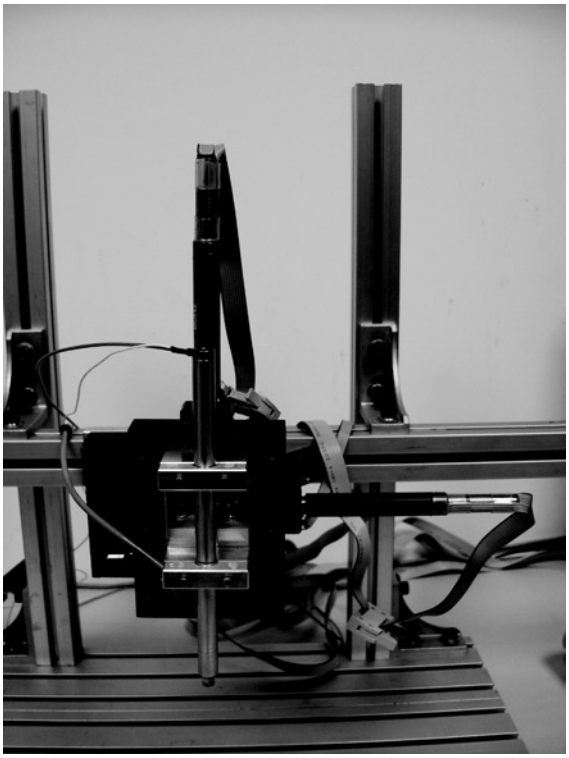

Fig. 17 *Photograph of the hardware device in implementing the tissue control method*

4 Experiments and results

4.1 System architecture for TCM

The new instrument that measures instantaneous blood pressure consists of hardware (Fig. 16) and the non-invasive estimation method. This instrument contains a Piezo-actuator actuating a pressure transducer to maintain the mean blood pressure and to track the variation of the blood pressure and a strain gauge attached on the actuator to measure the variation in blood vessel diameter. The compliance transducer head mounts on the skin to press down the pressure transducer with the attached actuator and to sense the pressure and displacement signals. The movement

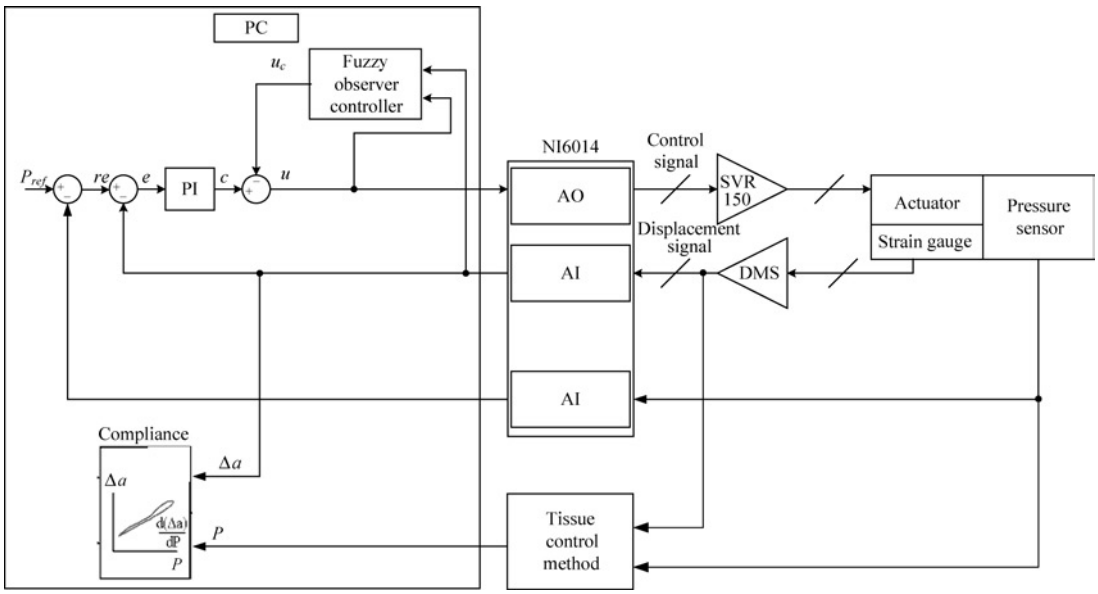

Fig. 16 *Schematic block diagram of implementing the tissue control method*

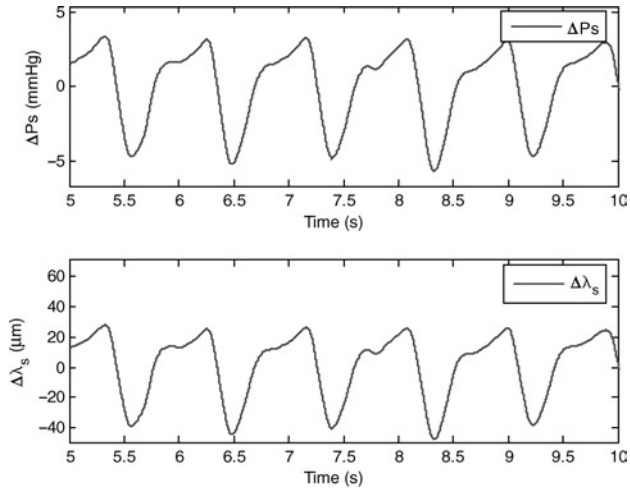

Fig. 18 *Actuating pressure and the variation of blood vessel diameter*

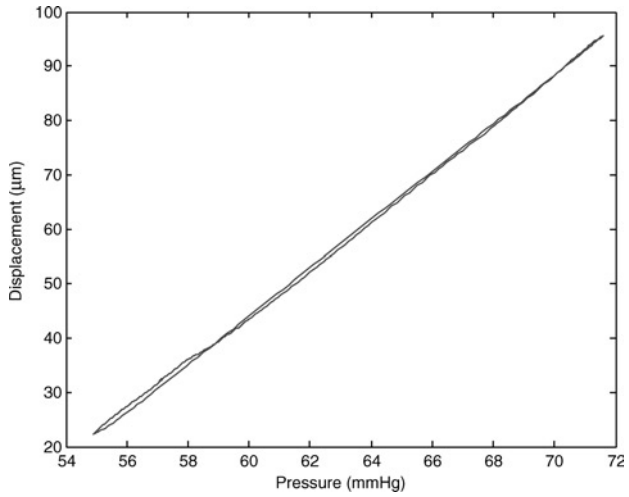

Fig. 19 *Compliance chart corresponding to Fig. 18*

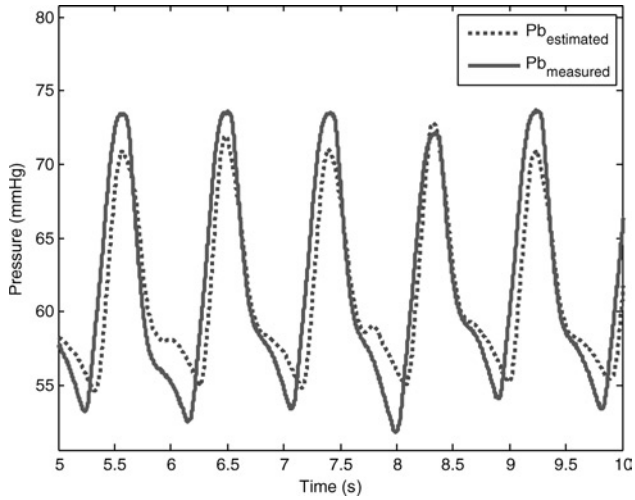

Fig. 20 *Measured and estimated instantaneous blood pressures*

is actuated by a piezo-actuator PST 150/5 made by Piezolechanhk, Inc., with 100 μm stroke, and a strain gauge is attached to the actuator. The fuzzy controller is mainly designed to linearise the hysteresis of the piezo-actuator and control the actuator to maintain the mean blood pressure. This controller has been tested and it was verified that the tracking capabilities were excellent within a response of 3 Hz, and it is capable of measuring the instantaneous arterial blood pressure. The photograph of the hardware device is shown in Fig. 17.

4.2 Experimental results

The instrument with the schematic block diagram shown in Fig. 16 was assembled and used in animal experiments conducted by the e-Med Biotech Inc. and ATIT [8]. Under room temperature, $24 \pm 1.5^{\circ}$C, six normal pigs with weight 35–40 kg were experimented with under anaesthesia. The blood pressure of the femoral artery was measured. A typical actuating pressure and the variation in blood vessel diameter from the animal test are shown in Fig. 18. Fig. 19 gives the corresponding compliance chart. Using (4) and (5), the instantaneous blood pressure is estimated and depicted in Fig. 19. The corresponding real and estimated blood pressures are shown Fig. 20, which is measured invasively by an additional pressure transducer (Grass Telfactor P10EZ). With respect to full scale, the average error of the estimated blood pressure is 0.2% and the maximum error is 8.75%. The comparison shows the average error is 1.60% for systolic blood pressure and 0.92% for diastolic blood pressure, respectively. This shows a satisfactory result.

5 Conclusion

This paper presents a fuzzy controller design for an instrument that measures the variation in blood vessel diameter and estimates the instantaneous arterial blood pressure via TCM. With the aid of the system identification technique, the nonlinear Bouc–Wen model for the hysteresis behaviour of piezo-actuator's movement is built and transferred into the T–S fuzzy model with approximated affine linear behaviour. On the basis of the fuzzy model, a robust observer is designed to linearise the hysteresis behaviour. A PI controller is also designed to track the variation in blood pressure. We combine these two parts into a fuzzy controller for controlling the motion of the piezo-actuator. After software and hardware verification tests, there is still some delay effect that contributes to discrepancies between the expected and actual output signals. A Fourier series analysis is used to reduce the discrepancies via delay-time compensation. Finally, the instrument with the proposed fuzzy controller is used in animal experiments. The experiments show that the designed fuzzy controller is feasible and presents satisfactory results for estimating the instantaneous blood pressure.

6 Acknowledgment

The authors would like to express gratitude to e-Med Biotech, Inc. for financial and technical support. In consequence, e-Med Biotech, Inc. reserves all rights to the patent of the instantaneous arterial blood pressure measuring system.

7 References

1 Geddes, L.A., Voelz, M., James, S., and Reiner, D.: 'Pulse arrival time as a method of obtaining systolic and diastolic blood pressure indirectly', *Med. Biol. Eng. Comput.*, 1981, **19**, (5), pp. 671–672

2 Talke, P.O.: 'Measurement of systolic blood pressure using pulse oximetry during helicopter flight', *Crit. Care Med.*, 1991, **19**, (7), pp. 934–937

3 Kurozawa, Y., Nasu, Y., and Oshiro, H.: 'Finger systolic blood pressure measurements after finger cooling', *J. Occup. Med.*, 1992, **34**, (7), pp. 683–686

4 Sharir, T., Marmor, A., Ting, C.-T., Chen, J.-W., Liu, C.-P., Chang, M.-S., Yin, F.C., and Kass, D.A.: 'Validation of a method for noninvasive measurement of central arterial pressure', *Hypertension*, 1993, **21**, (1), pp. 74–82

5 Fronek, A., Blazek, V., and Curran, B.: 'Toe pressure determination by audiophotoplethysmography', *J. Vasc. Surg.*, 1994, **20**, (2), pp. 267–270

6 Yamakoshi, K.: 'Non-invasive cardiovascular hemodynamic measurements', Öberg, P.A., Togawa, T., and Spelman, F.A. (Eds.): 'Sensors in medicine and heath care' (Wiley-VCH Verlag GmbH & Co. KGaA, 2004), pp. 107–160

7 Tanaka, S., Gao, S., Nogawa, M., and Yamakoshi, K.-I.: 'Noninvasive measurement of instantaneous radial artery blood pressure', *IEEE Eng. Med. Biol. Mag.*, 2005, **24**, (4), pp. 32–37

8 Lin, A.C.-Y., Huang, H.-N., Su, Y.-C., *et al.*: 'On measuring the instantaneous blood pressure in the artery via tissue control method', *Physiol. Meas.*, 2007, **28**, pp. 937–951

9 Wen, Y.K.: 'Method for random vibration of hysteretic systems', *J. Eng. Mech. Division, ASCE*, 1976, **102**, (2), pp. 249–263

10 Takagi, T., and Sugeno, M.: 'Fuzzy identification of systems and its applications to modeling and control', *IEEE Trans. Syst. Man Cybernet.*, 1985, **15**, (1), pp. 116–132

11 Tanaka, K., and Wang, H.O.: 'Fuzzy control systems design and analysis: a linear matrix inequality approach' (John Wiley & Sons, Inc., 2001)

12 Boyd, S., El Ghaoui, L., Feron, E., and Balakrishnan, V.: 'Linear matrix inequalities in systems and control theory' (SIAM, 1994)

13 Balas, G., Chiang, R., Packard, A., and Safonov, M.: 'Robust control toolbox user's guide' (The MathWorks, Inc., 2005, 3rd edn.)